OMTN, Volume *21*

Supplemental Information

Dissecting the Functional Mechanisms of Somatic Copy-Number Alterations Based on Dysregulated ceRNA Networks across Cancers

Yanyan Ping, Yao Zhou, Jing Hu, Lin Pang, Chaohan Xu, and Yun Xiao

Supplemental Figures

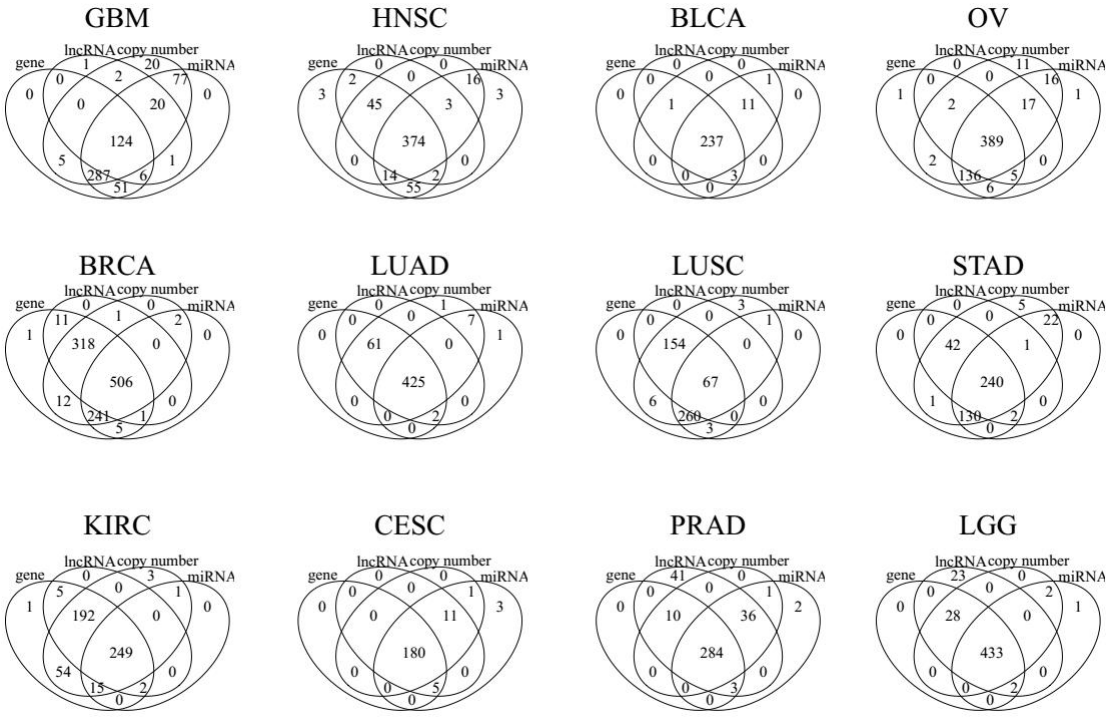

Figure S1. The overlaps of tumor patients among expression profiles of lncRNA, PGs and miRNAs and copy number profiles in 12 cancer types.

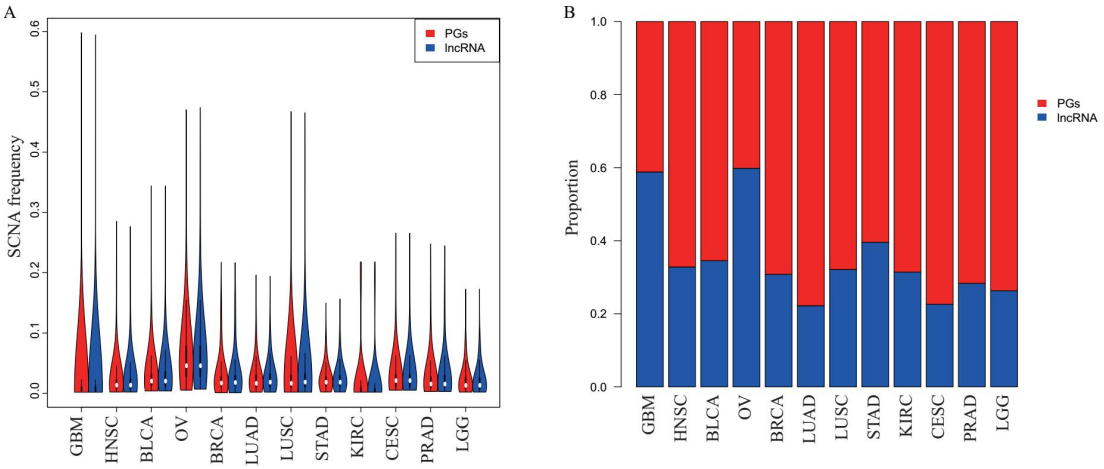

Figure S2. The SCNAs of LncRNA were prevailing in cancers. **A.** The SCNA frequencies of PGs and lncRNAs across cancers. **B.** The proportions of PGs and lncRNAs in candidate genes cross 12 cancer types.

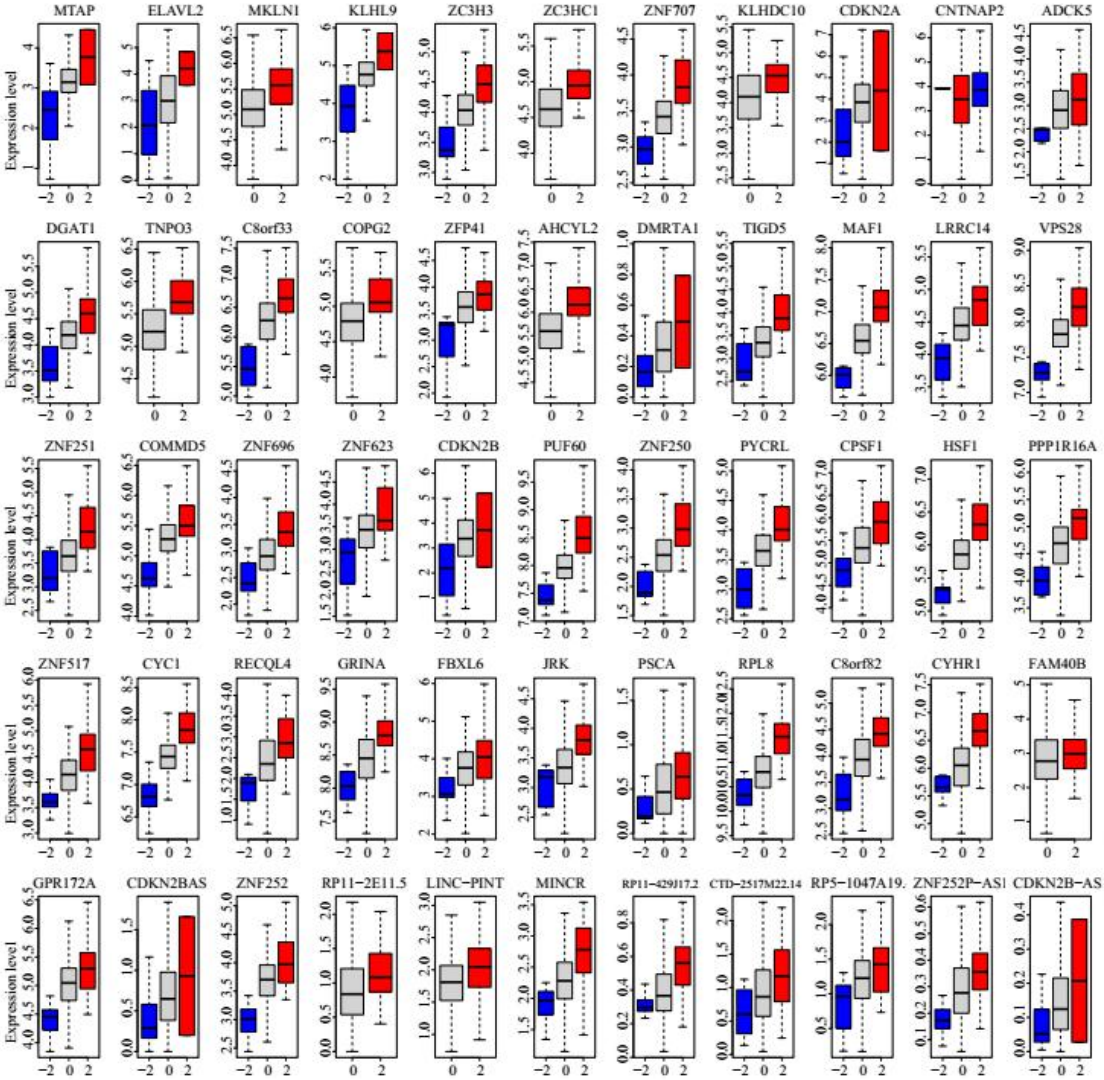

Figure S3. SCNAs of 55 candidate genes significantly and accordantly influenced their expression levels in LGG. -2 represents for homozygous deletion (blue), 0 for non-alteration (gray) and 2 for high-level amplification (red).

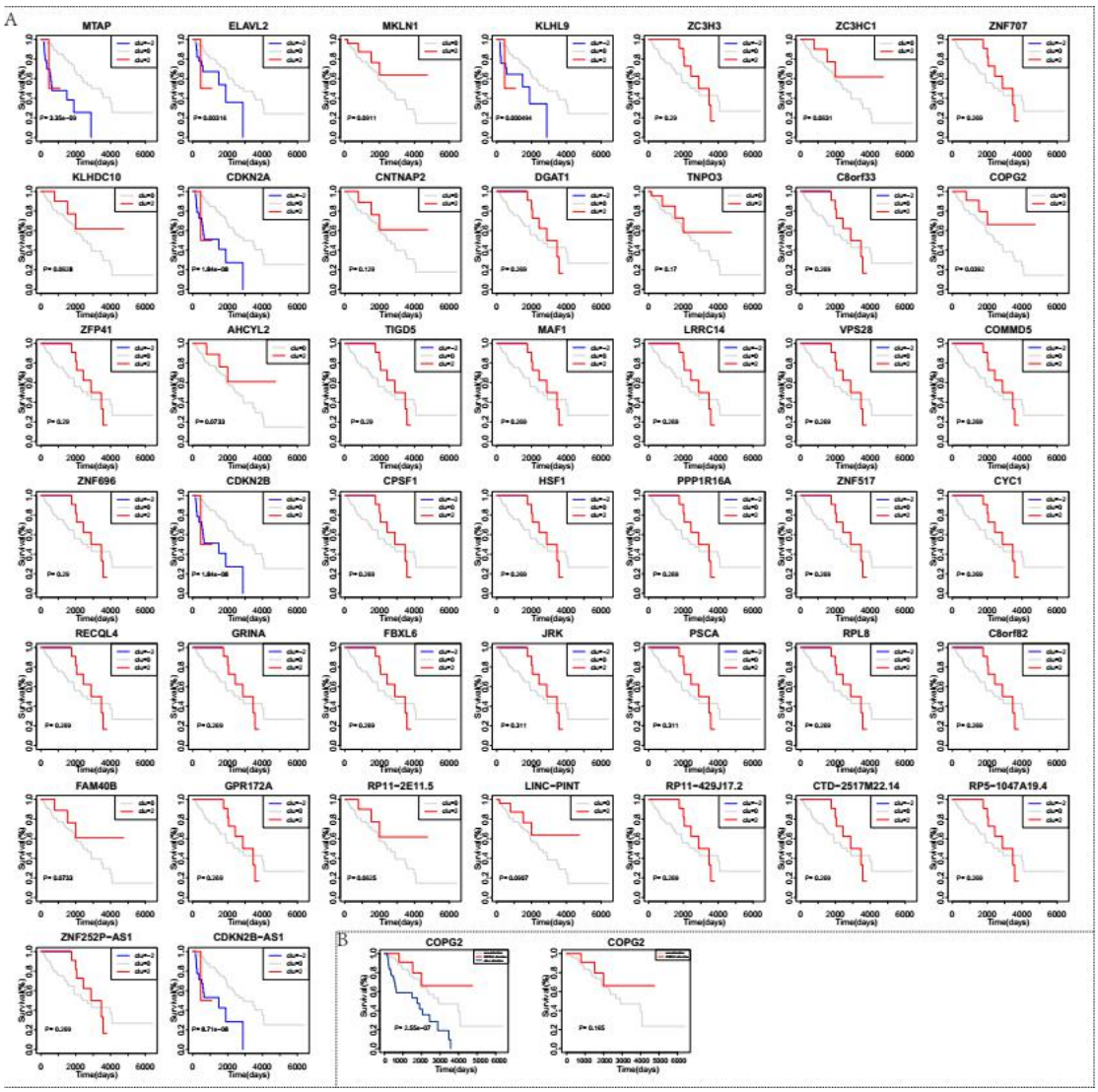

Figure S4. Survival analysis of 44 driver genes in LGG. A. The associations of SCNA status of 44 driver genes with LGG prognosis. -2 represents for homozygous deletion (blue), 0 for non-alteration (gray) and 2 for high-level amplification (red). B. COPG2 amplification was not an independent prognostic factor in LGG.

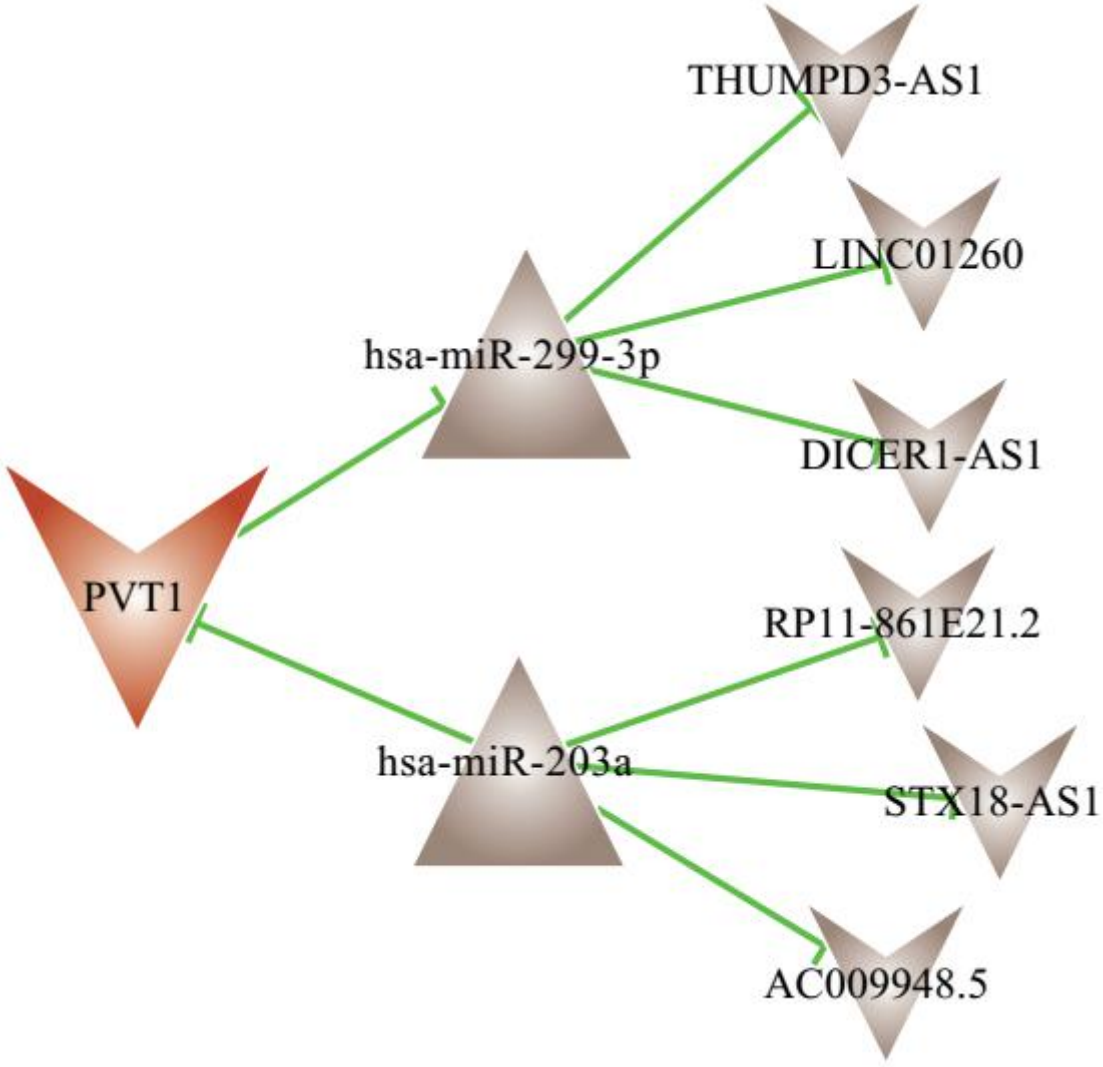

Figure S5. PVT1 amplification-driven dysregulated ceRNA network in OV.

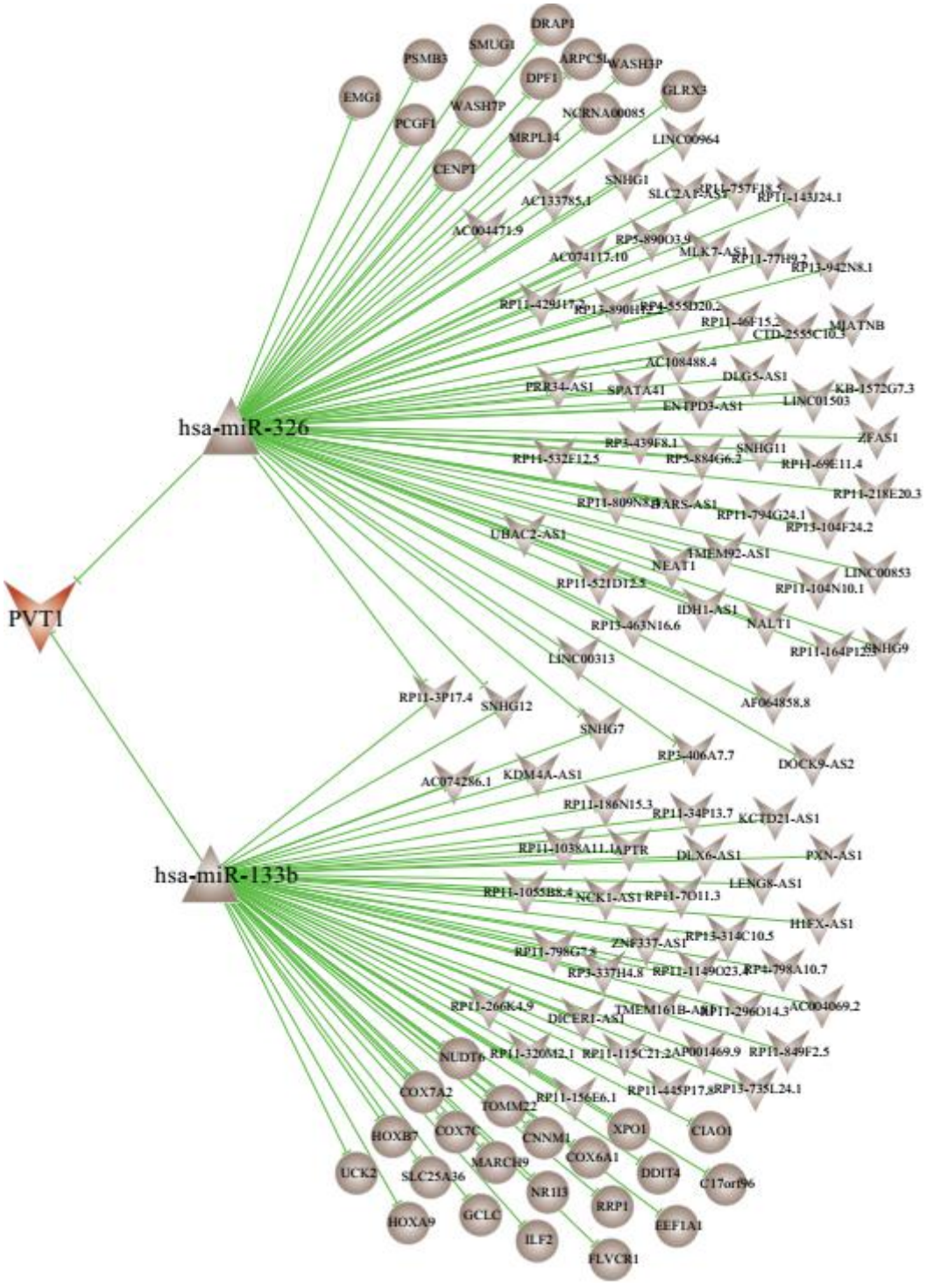

Figure S6. PVT1 amplification-driven dysregulated ceRNA network in HNSC.

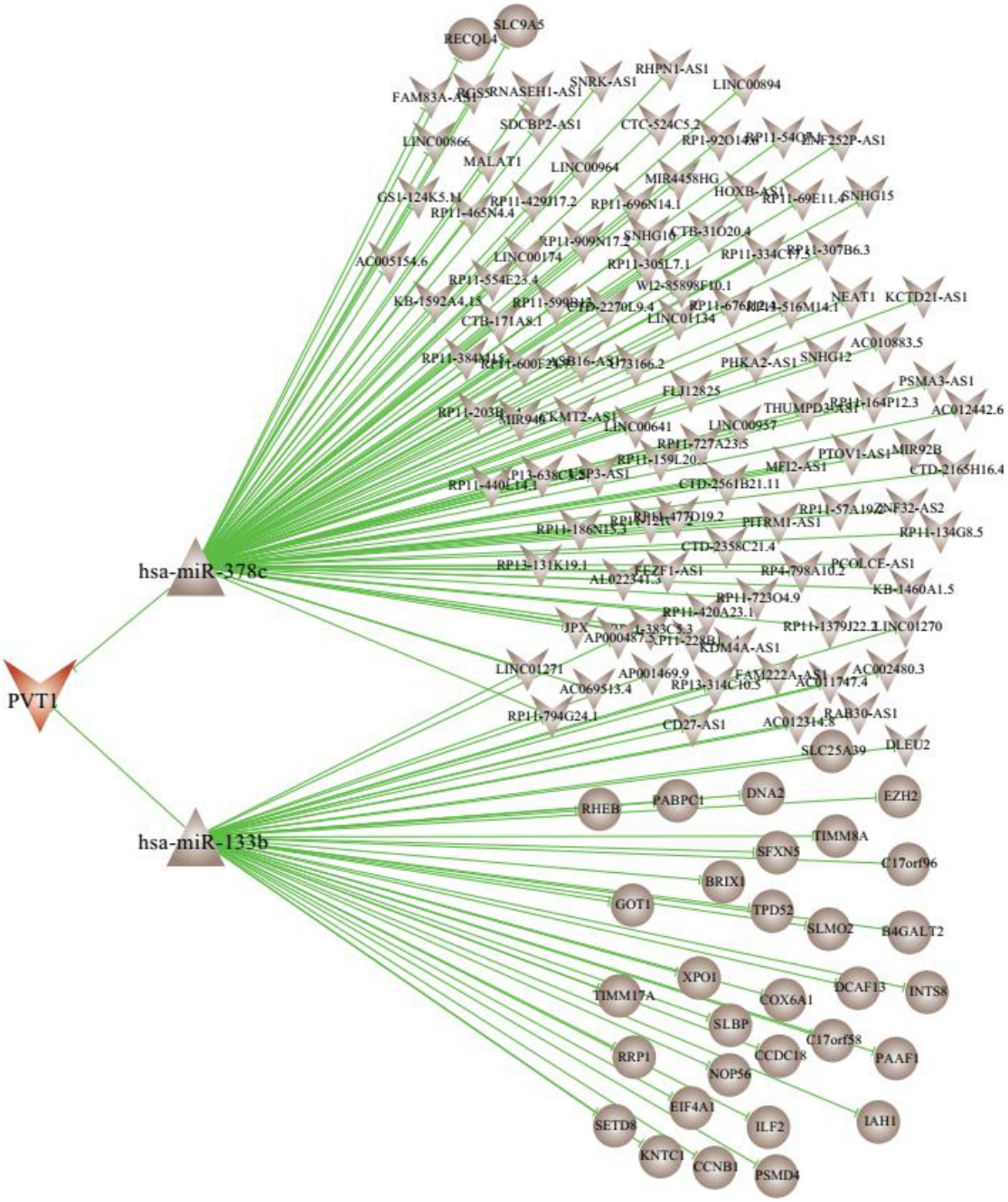

Figure S7. PVT1 amplification-driven dysregulated ceRNA network in LUAD.

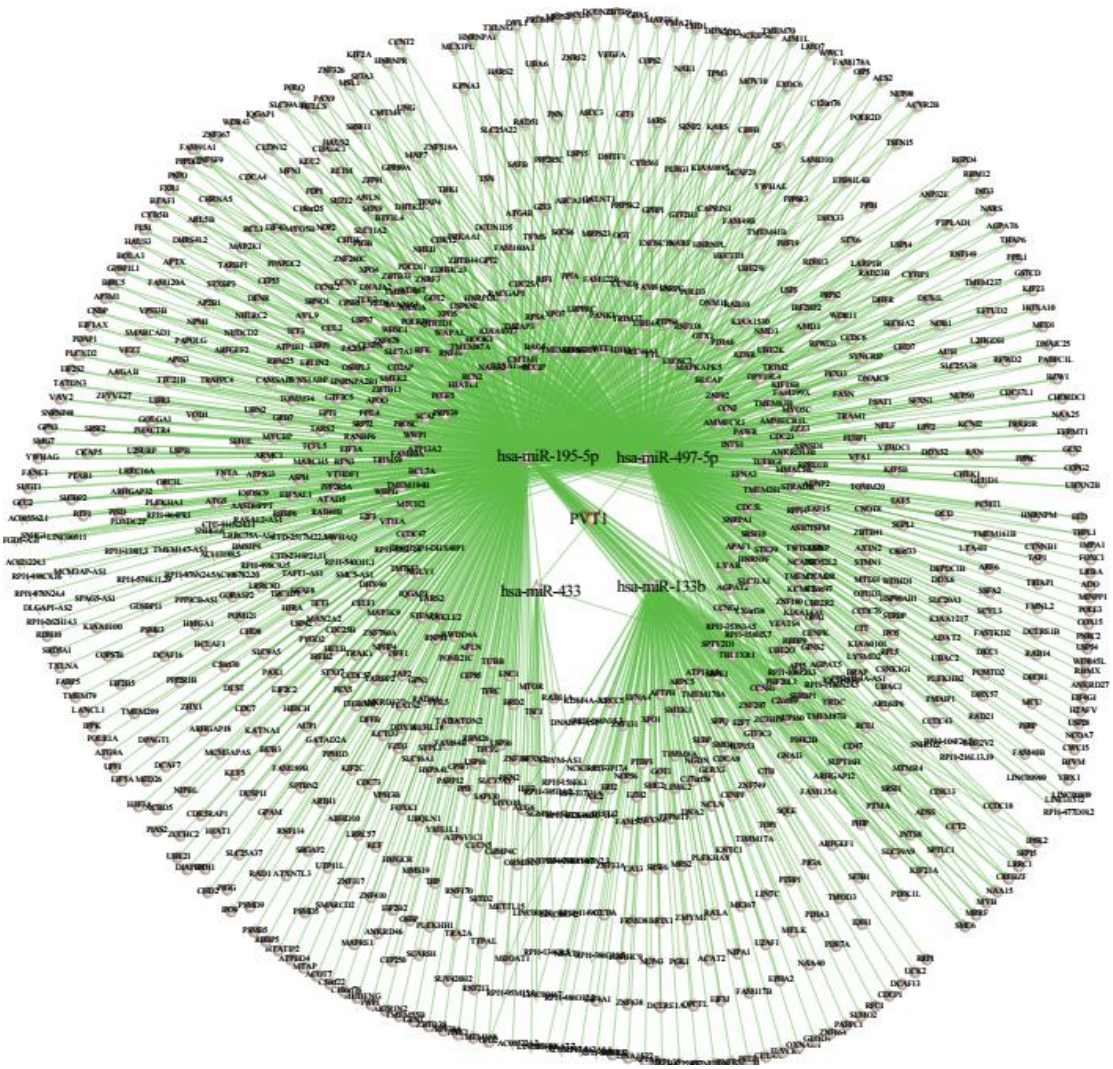

Figure S8. PVT1 amplification-driven dysregulated ceRNA network in STAD.

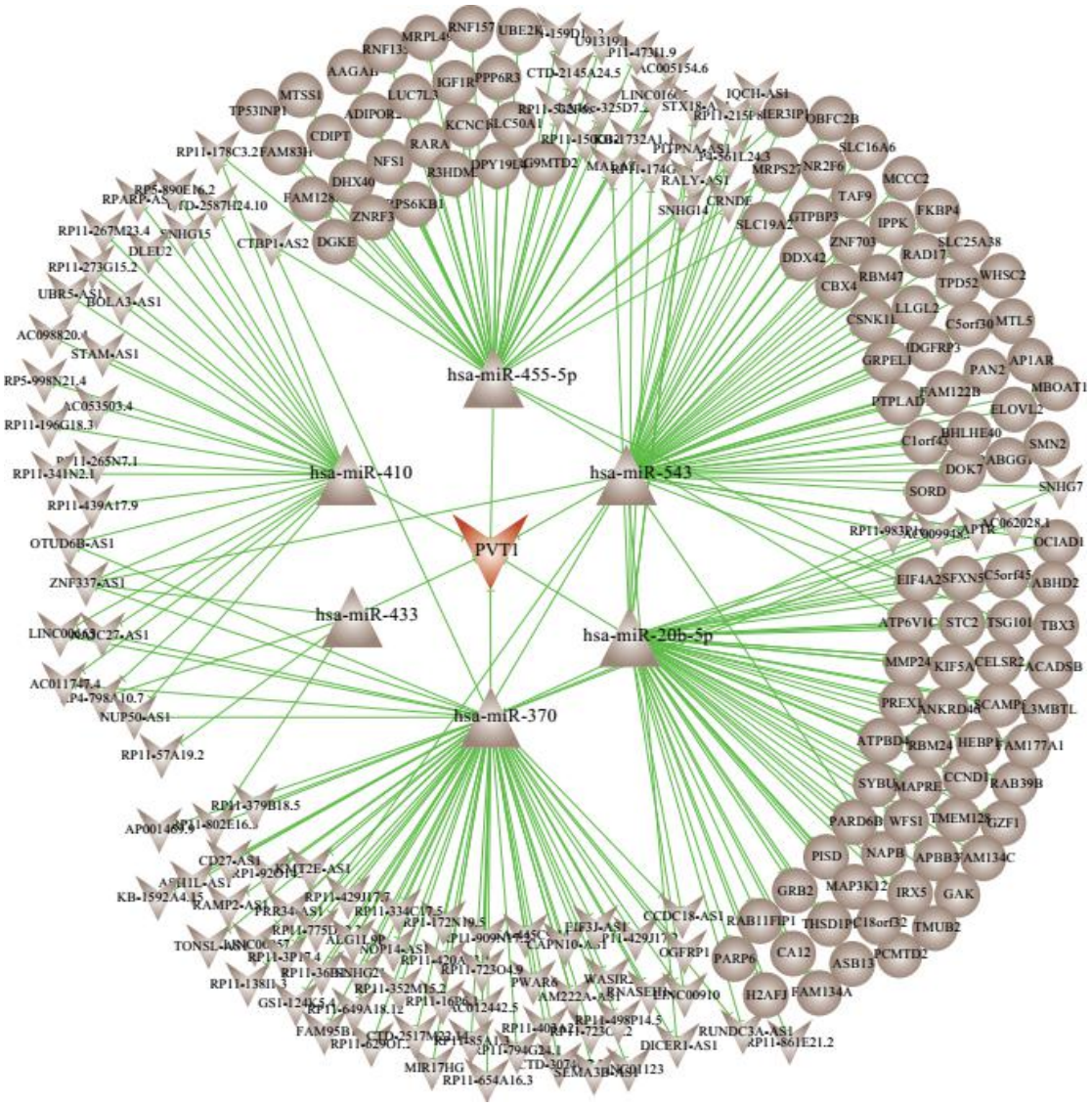

Figure S9. PVT1 amplification-driven dysregulated ceRNA network in BRCA.

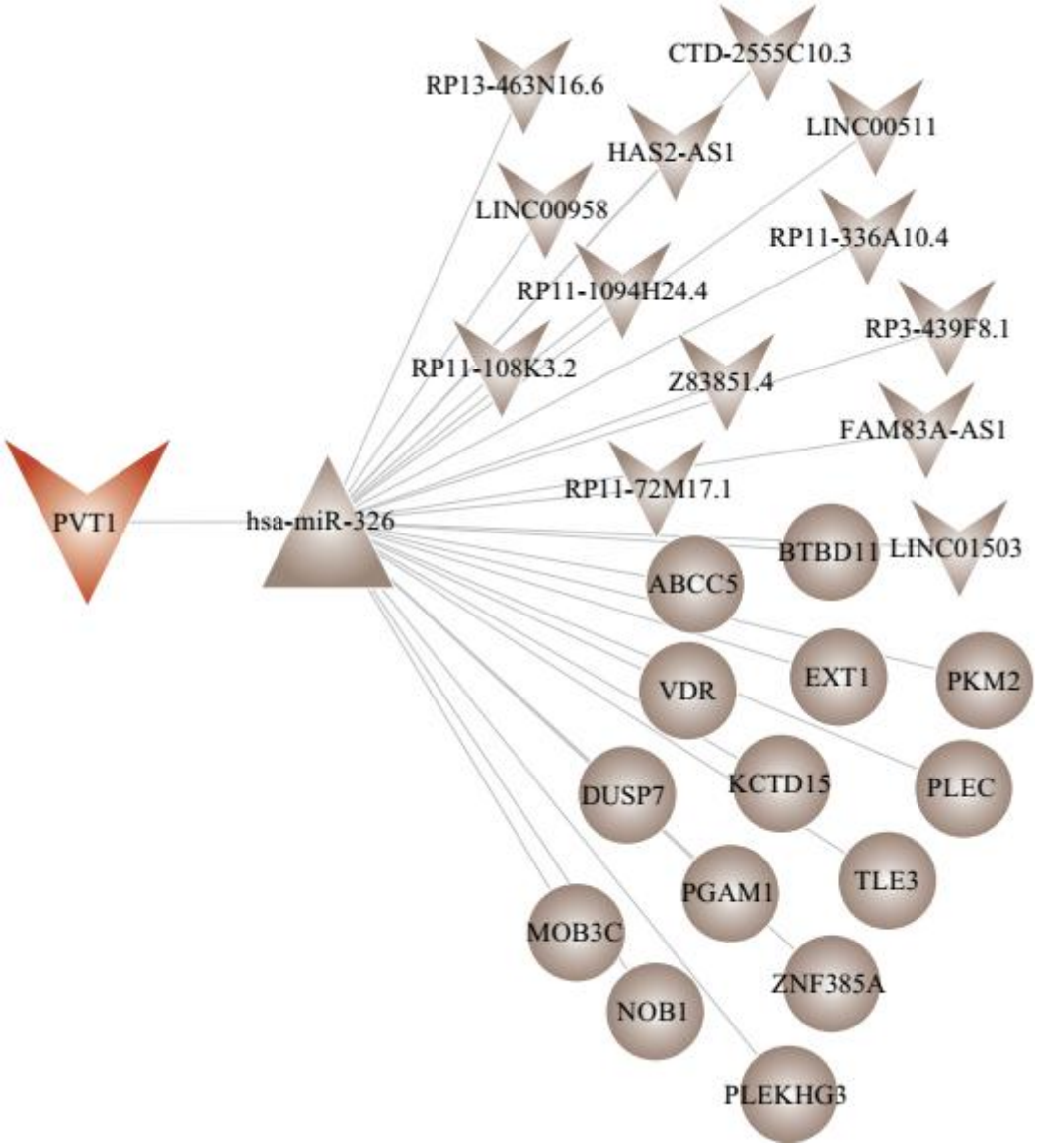

Figure S10. PVT1 amplification-driven dysregulated ceRNA network in BLCA.

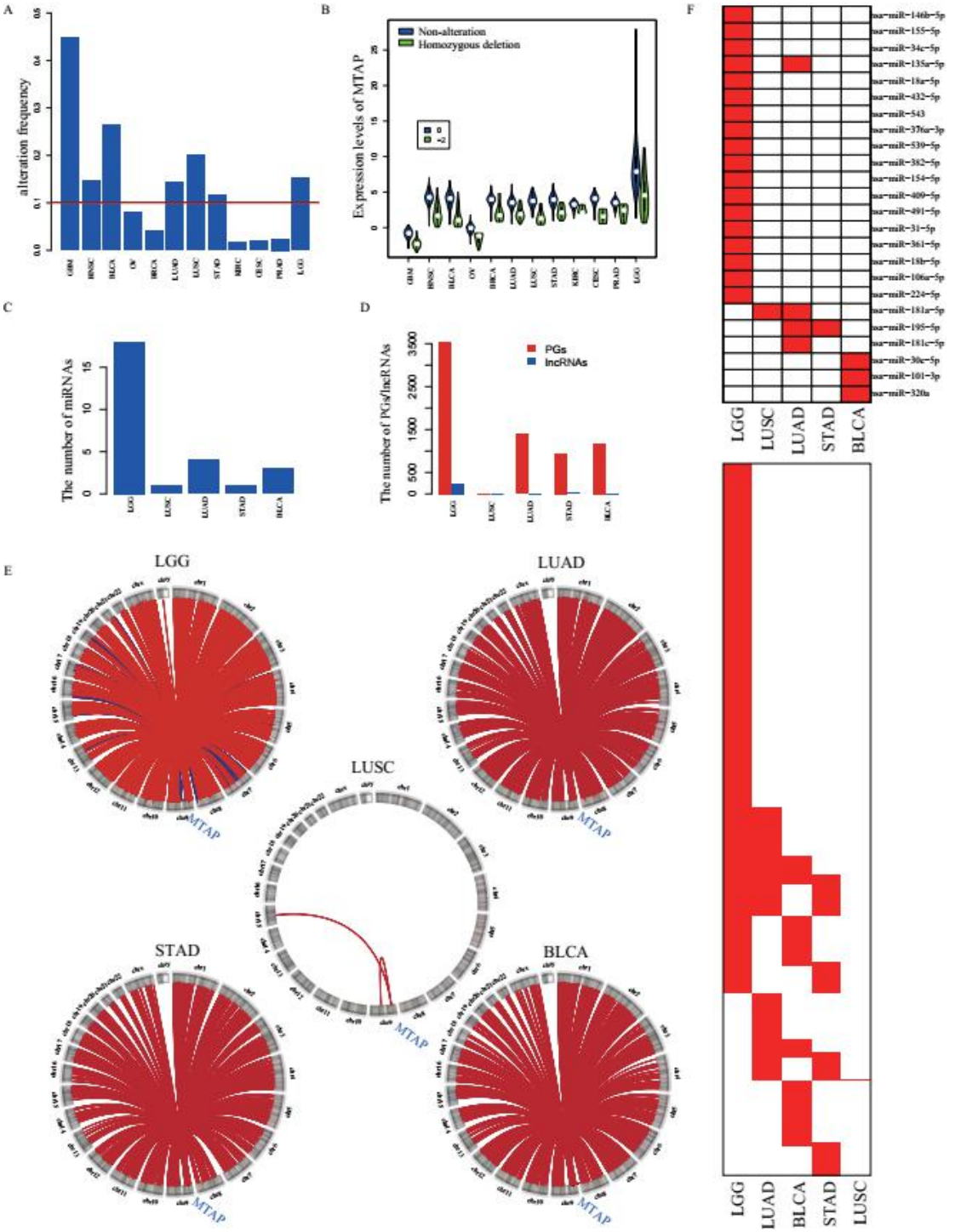

Figure S11. Homozygous deletion of MTAP disturbed distinct different ceRNA networks in different cancers. A. Alteration frequency of MTAP in 12 cancer types. B. Homozygous deletion of MTAP significantly down-regulated the MTAP expression levels in 12 cancer types. C. The numbers of miRNAs in MTAP homozygous deletion-induced dysregulated ceRNA networks in five types of cancers including LGG, LUSC, LUAD, STAD, BLCA. D. The numbers of PGs and lncRNAs in MTAP-mediated dysregulated ceRNA networks in five types of cancers. E. Genome-wide view of

active ceRNA partners of MTAP in different cancers. Blue, lncRNA; Red, PGs. F. Heatmap for miRNAs in MTAP-mediated dysregulated ceRNA networks in five types of cancers. G. Heatmap for ceRNAs of MTAP in MTAP-mediated dysregulated ceRNA networks in five types of cancers.

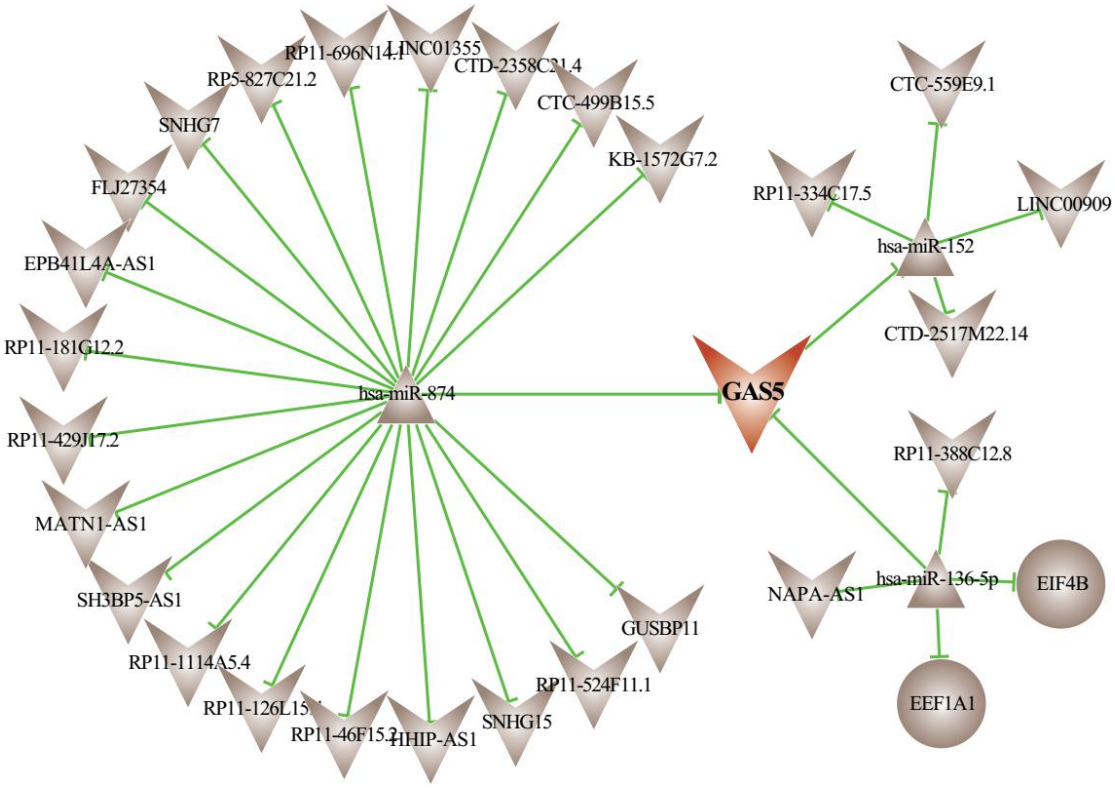

Figure S12. GAS5 amplification-driven dysregulated ceRNA network in BRCA.

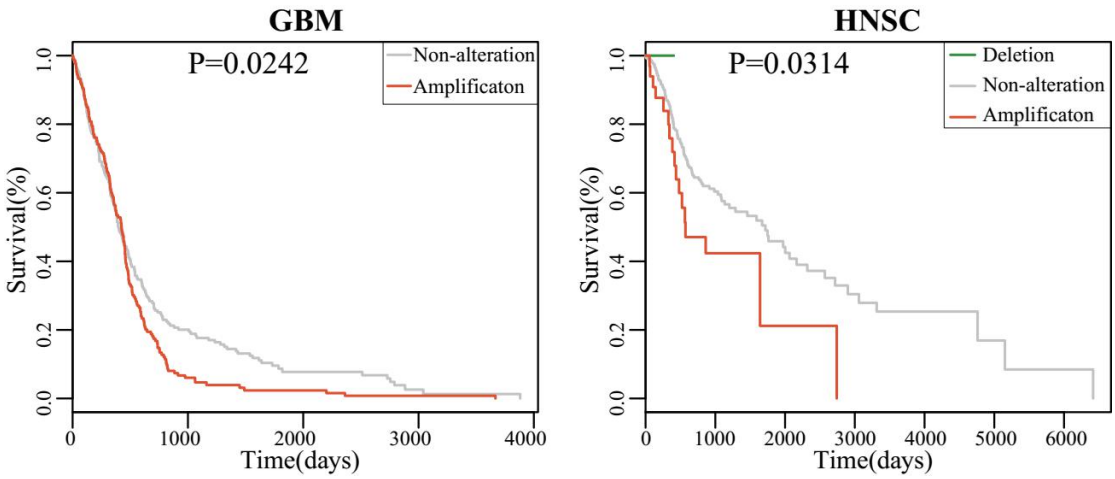

Figure S13. The EGFR amplification were associated with poor prognosis of GBM and HNSC.

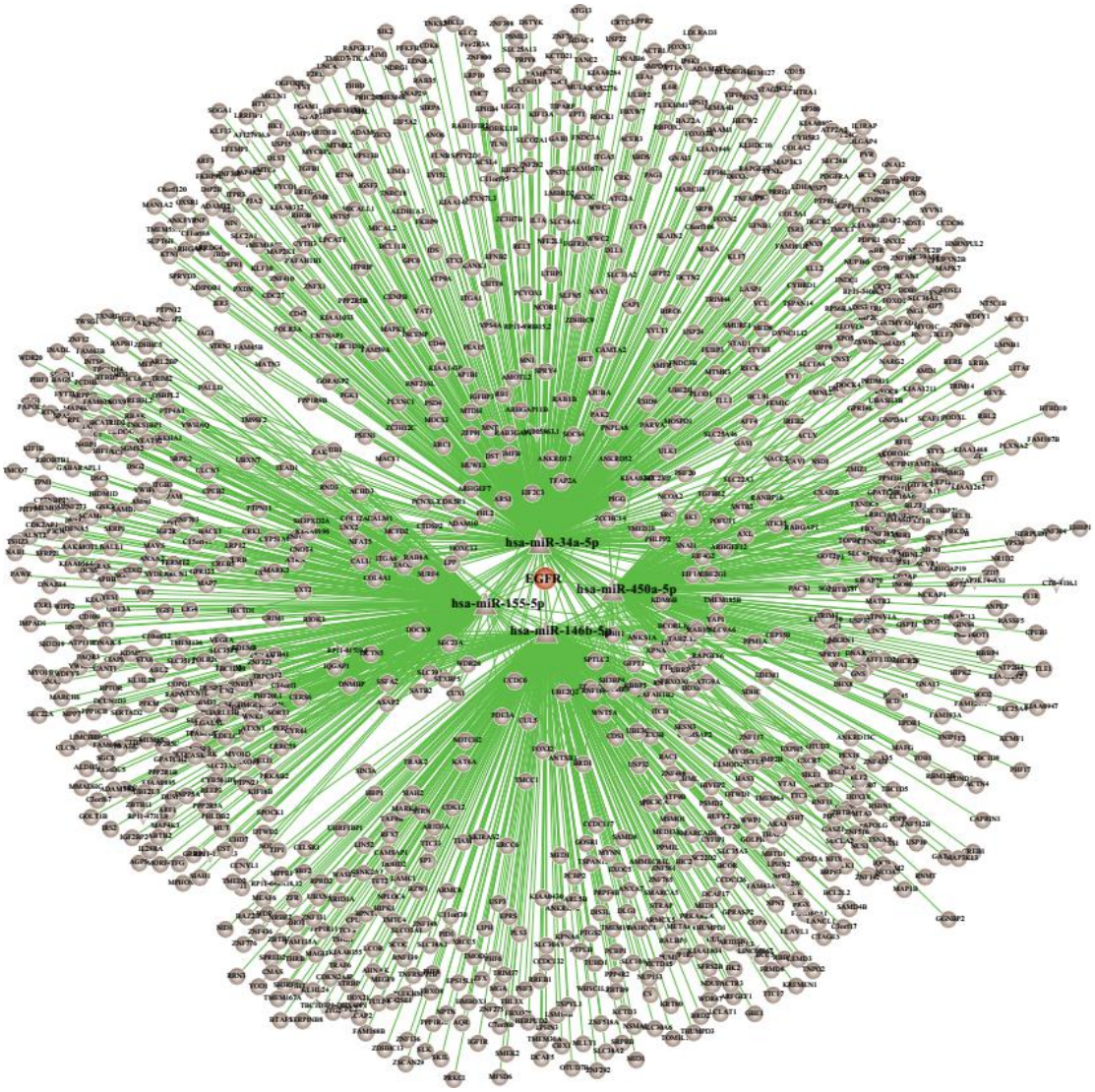

Figure S14. EGFR amplification-driven dysregulated ceRNA network in HNSC.

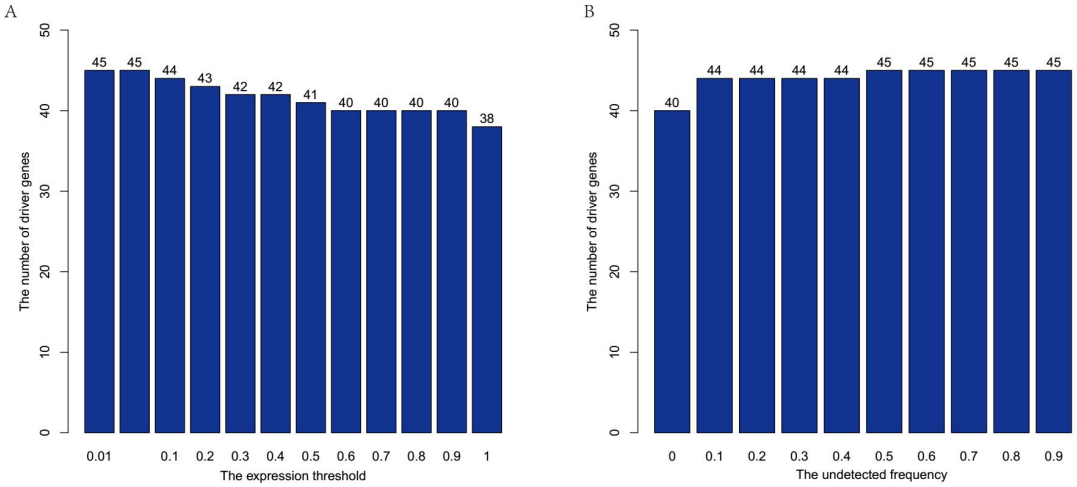

Figure S15. The influence of thresholds of mean expression and undetected frequency on the method for identifying driver genes. A. The number of driver genes identified at different threshold of mean expression. B. The number of driver genes identified as different threshold of undetected frequency.

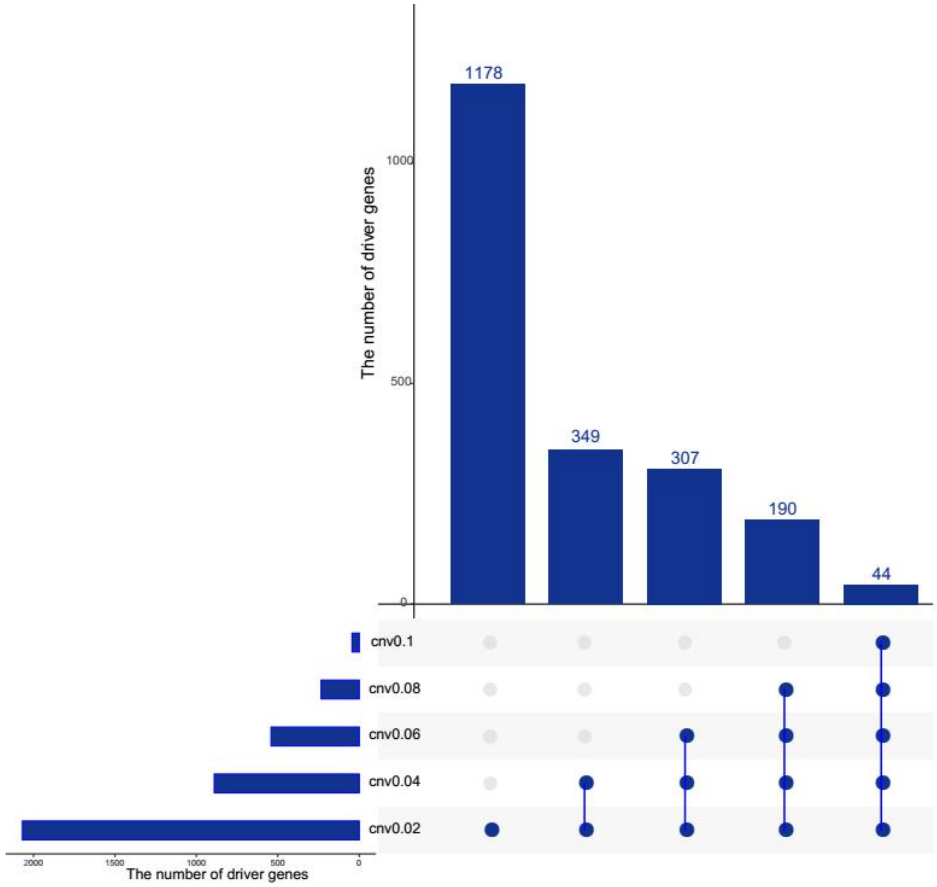

Figure S16. The overlaps of driver genes identified by our method at different thresholds of SCNA frequencies.

Supplemental Table

Table S1. The numbers of cancer samples in copy number profiles and expression profiles of PGs, lnvRNAs and miRNAs for 12 cancer types

Cancer type	Expression profiles			Copy number profiles	Common samples
	PG	lncRNA	miRNA		
GBM	473	154	571	535	124
HNSC	495	426	467	452	374
BLCA	241	252	252	250	237
LUAD	488	488	482	494	425
OV	541	412	585	572	389
BRCA	1095	837	755	1080	506
LUSC	490	220	331	490	67
STAD	415	285	395	441	240
KIRC	518	448	267	514	249
CESC	185	196	200	192	180
PRAD	297	374	326	331	284
LGG	463	486	438	463	433
Total	5701	4578	5069	5814	3508